IJASST International Journal of Applied Sciences and Smart Technologies

Volume 06
Issue 01

p-ISSN 2655-8564, e-ISSN 2685-943, pp. 99-112, 2024

Design of Maximum Torque Per Ampere Control Method In Squirrel CageThree-Phase Induction Motor

Regina Chelinia Erianda Putri[1*], Feri Yusivar [2]

[1]*Faculty of Science and Technology, Sanata Dharma University, Yogyakarta, 55281, Indonesia*
[2] *Faculty of Engineering, University of Indonesia, Depok, 16424, Indonesia*
[*]*Corresponding Author: regina.chelinia@usd.ac.id*

(Received 23-10-2023; Revised 19-01-2024; Accepted 25-04-2024)

Abstract

Improving the performance of three-phase induction motors is currently carried out by various control methods. One of them is controlling a three-phase induction motor using the Maximum Torque Per Ampere (MTPA) method. This paper focuses on the study of modeling specific motor models using the MTPA method. The purpose of the study is to prove that with the squirrel cage motor model, the speed can be increased above its rating. The MTPA method is a method of controlling a three-phase induction motor by controlling the current from the torque speed. Modeling is tested to see the responsiveness of the modeled system. The experimental results were tested using two-speed references and the system showed that MTPA control induction motors can improve the performance of three-phase induction motors. The results from the design show that the MTPA method can increase the performance of three-phase induction motors to reach 84.4%. The results of this study can be used as one way to model induction motors.
Keywords: Induction Motor, Modelling, MTPA

1 Introduction

Developments in the field of transportation in the current era are growing rapidly. However, it is not balanced with waste treatment, making the environment polluted with smoke pollution. According to the results of the study "In the last 100 years the earth has increased in temperature up to 0.18 degrees Celsius" [1].

The transition from fossil fuel energy to electrical energy as energy in the field of transportation requires one component of electric vehicle design, namely the induction motor. Induction motor is the leading technology in many industrial applications, nevertheless, suitable IM designs are proposed even for automotive applications[2]. A

This work is licensed under a Creative Commons Attribution 4.0 International License

three-phase induction motor is an electronic device that aims to convert electrical energy into mechanical energy. A widely used induction motor is a three-phase induction motor known as an asynchronous motor, called because of the difference in speed from the rotation of the rotor to the rotation speed of the stator.

There are several ways to improve motor capabilities above the rate discussed in previous studies. MTPA Method has several various developments such as the title Direct Quadrate (D-Q) Modeling in the Speed Control System of Three Phase Induction Motors With Field Oriented Control (FOC) Based on P-I Controlled [3] study discusses controlling induction motors with FOC based on PI controllers. Speed Sensorless Control of Parallel Connected Dual Induction Motor Fed by Single Inverter using Direct Torque Control [4] discusses controlling two induction motors with parallel induction motors. Another research titled Comparative Performance of Induction Motor Speed Controller System with Flux Weakening Control discusses the purpose of controlling iq^* by limiting where there is $|iq|$ input [5].

The purpose of this study is to prove that with certain motor models, speed can be increased above its rating. The MTPA method is a three-phase induction motor control method by adjusting the reference input of torque current and flux current to control the rotational speed of the induction motor. Recently, the maximum torque per ampere (T/A) scheme has been proposed to minimize the stator current and reduce inverter losses [6]. Neither “minimum loss” nor “maximum torque per ampere” provided optimal motor drive performance and that drive performance was optimal between the two conditions [7]. MTPA is designed to ensure that the current used is the minimum i_d current for development at motor torque, with the total stator flux controlled by the MTPA criterion.

2 Research Method

The system uses models and methods, namely induction motor models, Clark-Park transformation methods, Rotor Field Oriented Control (RFOC), and MTPA modeling.

A. Induction motor model

Induction motor modeling uses the stator voltage vector $(v_s)'$, the stator current vector $(i_s)'$, the stator flux vector $(\psi_s)'$ and the rotor flux vector $(\psi_r)'$. The general equation of the induction motor is as follows.

$$\overrightarrow{V_s}' = R_s\overrightarrow{\imath_s}' + \frac{d}{dt}\overrightarrow{\psi_s}' + j\omega_e\overrightarrow{\psi_s} \quad \textit{(Eq. 1)}$$

$$\overrightarrow{V_r}' = R_r\overrightarrow{\imath_r}' + \frac{d}{dt}\overrightarrow{\psi_r}' + j(\omega_e - \omega_r)\overrightarrow{\psi_r} \quad \textit{(Eq. 2)}$$

$$\overrightarrow{\psi_s}' = L_s\overrightarrow{\imath_s}' + L_m\overrightarrow{\imath_r}' \quad \textit{(Eq. 3)}$$

$$\overrightarrow{\psi_r}' = L_r\overrightarrow{\imath_r}' + L_m\overrightarrow{\imath_s}' \quad \textit{(Eq. 4)}$$

B. Clark-Park Transformation

The induction motor used is a three-phase induction motor, but modeling is carried out in two phases which aims to simplify calculations and analysis. Transformation from three phases to two phases, the transformations used are Clarke Transformation and Park Transformation. [8]

The Clarke transform is a transformation that transforms a system that is on the (abc axis) into a stationary state frame of reference ($\alpha\beta$ axis). In the stator frame of reference, $\omega_e = 0$ and then in the cage rotor type, the terminals are briefly connected so that the rotor voltage is $V_r = 0$. The substitution of the equation of stator current and rotor current obtained induction motor model in the $\alpha\beta$ axis becomes,

$$\frac{d}{dt}i_{s\alpha} = \left(-\frac{R_s}{\sigma L_s} - \frac{(1-\sigma)}{\sigma\tau_r}\right)i_{s\alpha} + \frac{L_m}{\sigma L_s L_r \tau_r}\psi_{r\alpha} + \frac{L_m\omega_r}{\sigma L_s L_r}\psi_{r\beta} + \frac{1}{\sigma L_s}V_{s\alpha} \quad \textit{(Eq. 5)}$$

$$\frac{d}{dt}i_{s\beta} = \left(-\frac{R_s}{\sigma L_s} - \frac{(1-\sigma)}{\sigma\tau_r}\right)i_{s\beta} - \frac{L_m\omega_r}{\sigma L_s L_r}\psi_{r\alpha} + \frac{L_m}{\sigma L_s\tau_r L_r}\psi_{r\beta} + \frac{1}{\sigma L_s}V_{s\beta} \quad \textit{(Eq. 6)}$$

$$\frac{d}{dt}\psi_{r\alpha} = \frac{R_r}{L_r}L_m i_{s\alpha} - \frac{R_r}{L_r}\psi_{r\alpha} - \omega_r\psi_{r\beta} \quad \textit{(Eq. 7)}$$

$$\frac{d}{dt}\psi_{r\beta} = \frac{R_r}{L_r}L_m i_{s\beta} + \omega_r\psi_{r\alpha} - \frac{R_r}{L_r}\psi_{r\beta} \quad \textit{(Eq. 8)}$$

with $\sigma = \frac{L_s L_r - L_m^2}{L_s L_r}$ and $\tau_r = \frac{L_r}{R_r}$

Park transform is a transformation that transforms a two-phase system that is on a stationary frame of reference (αβ axis) transformed in a rotating frame of reference (dq axis). In the rotor frame of reference the location ω_e is put together by the axis of the rotor

causing the magnitude of ω_e is not equal to zero. The stator voltage transformation in equations (1)-(4) will be [9]:

$$\frac{d}{dt}i_{sd} = \left(-\frac{R_s}{\sigma L_s} - \frac{L_m^2}{\sigma L_s L_r \tau_r}\right) i_{sd} + \omega_e i_{sq} + \frac{L_m}{\sigma L_s L_r \tau_r}\psi_{rd} + \frac{L_m}{\sigma L_s L_r}\omega_r \psi_{rq} + \frac{1}{\sigma L_s} V_{sd}) \qquad \textit{(Eq. 9)}$$

$$\frac{d}{dt}i_{sq} = -\omega_e i_{sd} + \left(-\frac{R_s}{\sigma L_s} - \frac{L_m^2}{\sigma L_s L_r \tau_r}\right) i_{sq} - \frac{L_m}{\sigma L_s L_r}\omega_r \psi_{rd} + \frac{L_m}{\sigma L_s L_r \tau_r}\psi_{rq} + \frac{1}{\sigma L_s} V_{sq} \qquad \textit{(Eq.10)}$$

$$\frac{d}{dt}\psi_{rd} = \frac{R_r}{L_r} L_m i_{sd} - \frac{R_r}{L_r}\psi_{rd} + (\omega_e - \omega_r)\psi_{rq} \qquad \textit{(Eq. 11)}$$

$$\frac{d}{dt}\psi_{rq} = \frac{R_r}{L_r} L_m i_{sq} - (\omega_e - \omega_r)\psi_{rd} - \frac{R_r}{L_r}\psi_{rq} \qquad \textit{(Eq. 12)}$$

with, $\sigma = \frac{L_s L_r - L_m^2}{L_s L_r}$ and $\tau_r = \frac{L_r}{R_r}$ and rotor speed equation $\frac{d}{dt}\omega_r = \frac{T_e - T_i}{J}$:

While the mechanical equation of a motor that has a polar p-tide. In this case, electromagnetic torque T_e expressed by,

$$T_e = p\left(\frac{L_m}{L_r}\right)\left(i_{s\beta}\psi_{r\alpha} - i_{s\alpha}\psi_{\beta}\right) \qquad \textit{(Eq.13)}$$

$$T_e = p\left(\frac{L_m}{L_r}\right)\left(i_{sq}\psi_{rd} - i_{sd}\psi_{q}\right) \qquad \textit{(Eq. 14)}$$

The parameters used are as follows:

R_r = Resistance on the rotor (Ω)
R_s = Resistance on the stator (Ω)
L_m= Magnetic inductance (H)
L_s= Magnetic inductance (H)
L_r= Magnetic inductance (H)
σ = Leakage Coefficient
$i_{s\alpha}$ = α axis stator current (A)
$i_{s\beta}$ = β axis stator current (A)
i_{sd} = d-axis stator current(A)
i_{sq} = stator current q axis (A)
T_e = Electromagnetic torque (Nm)
T_l = Load torque (Nm)
$V_{s\alpha}$= Stator voltage on α axis (V)
$V_{s\alpha}$= Stator voltage on the β axis (V)
V_{sd}= Stator voltage on the d-axis (V)
V_{sq}= Stator voltage on the q-axis(V)
$\psi_{r\alpha}$ = Flux of α-axis rotor (Wb)
$\psi_{r\beta}$ = Flux of β-axis rotor (Wb)
ψ_{rd} = d-axis rotor flux (Wb)
ψ_{rq} = q-axis rotor flux (Wb)
ω_r = Rotor velocity (rad/s)
ω_e = Rotating field speed (rad/s)
p = number of poles or poles
τ_r = Rotor constant time

C. *Rotor Field Oriented Control* (RFOC)

The orientation of the FOC (Field Oriented Control) control used has three frames of reference, named the rotor-stator and the air gap. RFOC not require additional processes to separate the interrelationships of variables in the equation. Rotor-oriented FOC (RFOC) can separate (decoupling) flux and torque components so that they can be controlled by d-axis stator current (i_{sd}) and q-axis stator current (i_{sq}) respectively. The separation of the two components U_{sd} and U_{sq} is a linear part of the stator voltage after the decoupling process [10]. V_{cd} and V_{cq} are the non-linear part of the stator voltage after the decoupling process is carried out, as follows,

$$U_{sd} = R_s i_{sd} + L_s \sigma \frac{d}{dt} i_{sd} \quad \textit{(Eq. 15)}$$

$$U_{sq} = R_s i_{sq} + L_s \sigma \frac{d}{dt} i_{sq} \quad \textit{(Eq. 16)}$$

$$V_{cd} = -\sigma L_s \omega_e i_{sq} + \frac{L_m}{L_r} \frac{d}{dt} \psi_{rd} \quad \textit{(Eq. 17)}$$

$$V_{cq} = \sigma L_s \omega_e i_{sd} + \frac{L_m}{L_r} \omega_e \psi_{rd} \quad \textit{(Eq. 18)}$$

Then the current controller model is modeled as follows:

$$v_{sd}^* = -k_{idp} i_{sd} + k_{idp} i_{sd}^* + k_{idi} x_{sd} - \sigma L_s N \omega_m i_{sq1}^* - \sigma L_s \frac{R_r}{L_r} \frac{{i_{sq1}^*}^2}{i_{sd2}^*} \quad \textit{(Eq. 19)}$$

$$v_{sq}^* = -k_{iqp} i_{sq} + k_{iqp} i_{sq}^* + k_{iqi} x_{sq} + \sigma L_s N \omega_m i_{sd1}^* + \sigma L_s \frac{R_r}{L_r} \frac{i_{sd1}^* {i_{sq1}^*}^2}{i_{sd2}^*} + (1-\sigma) L_s N \omega_m i_{sd2}^* + \frac{(1-\sigma) L_s R_r}{L_r} i_{sq1}^* \quad \text{(Eq. 20)}$$

Where $k_{idp} = \frac{\sigma L_s}{T_d}$, $k_{idi} = \frac{R_s}{T_d}$, $k_{iqp} = \frac{\sigma L_s}{T_d}$, $k_{iqi} = \frac{R_s}{T_d}$

Further, the first order of the reference current of the slip frequency and decoupling calculation becomes,

$$\frac{d}{dt} i_{sd1}^* = \frac{1}{T_d} i_{sd}^* - \frac{1}{T_d} i_{sd1}^* \quad \textit{(Eq. 21)}$$

$$\frac{d}{dt} i_{sq1}^* = \frac{1}{T_d} i_{sq}^* - \frac{1}{T_d} i_{sq1}^* \quad \textit{(Eq. 22)}$$

$$\frac{d}{dt} i_{sd2}^* = \frac{1}{T_2} i_{sd}^* - \frac{1}{T_2} i_{sd2}^* \quad \textit{(Eq.23)}$$

D. MTPA Modelling

In fact, for designs produced with high-speed motors, increasing the current ratio limit allows achieving the same rated efficiency but with a lower slot area. This condition is suitable for inverter driven systems and optimized with the Maximum Torque per Ampere method. The maximum torque per ampere condition occurs when a certain torque

speed condition is achieved at the minimum stator current [11]. Normal rate speed electric motor will occur if the motor parameters from the real parameter. The process of the Maximum Torque Per Ampere Method in the MTPA condition process identified for a particular motor torque, the stator current components used are i_d and i_q. MTPA is operated under the condition of each d and q axis flux component in a synchronous reference frame using equations [12][13]. Flow-related signals are used to obtain information about the magnitude of the current that controls the flow. The energy stored in the magnetizing inductance remains constant.

The Maximum Torque Per Ampere method is shown in Fig. 1. The system is tested using Matlab – Simulink – Cmex. The component values of the d and q axes for the flux synchronous reference frame for the MTPA method are given by the equation.

$$\psi_{ds}|_{TMPA} = \frac{L_s}{L_m}\sqrt{\frac{2T_e L_r}{P}} \qquad \textit{(Eq. 24)}$$

$$\psi_{qs}|_{TMPA} = \frac{\sigma L_s}{L_m}\sqrt{\frac{2T_e L_r}{P}} \qquad \textit{(Eq. 25)}$$

The values of the total flux components on the d and q axes in the synchronous reference frame are shown as

$$|\overrightarrow{\psi_s}|_{TMPA} = \frac{L_s}{L_m}\sqrt{\frac{2L_r\,(1+\sigma^2)T_e}{P}} \qquad \textit{(Eq. 26)}$$

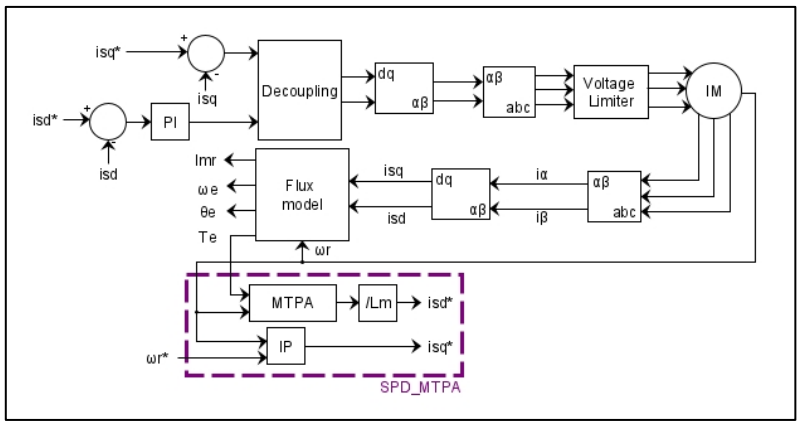


Figure 1 . Block Process Diagram MTPA Method

Then substitute $\omega_{sl} = \frac{R_r}{L_r}\frac{i^*_{sq1}}{i^*_{sd2}}$, $v_{sd} = v^*_{sd}$, and $v_{sq} = v^*_{sq}$, $|\psi_s| = \frac{L_s}{L_m}\sqrt{\frac{2L_r(1+\sigma^2)i^*_{sq}}{P}}$ so $i^*_{sd} = 1 + \frac{L_s}{L^2_m}\sqrt{\frac{2L_r(1+\sigma^2)i^*_{sq}}{P}}$

The modeling results that have been linearized into,

$$\frac{d}{dt}\Delta i_{sd} = \left(-\frac{k_{idp}+R_s}{\sigma L_s} - \frac{R_r(1-\sigma)}{\sigma L_r}\right)\Delta i_{sd} + \left(N\omega_{m0} + \frac{R_r i^*_{sq10}}{L_r i^*_{sd20}}\right)\Delta i_{sq} + \left(\frac{L_m R_r}{\sigma L_s L_r^2}\right)\Delta\psi_{rd} + \left(\frac{NL_m\omega_{m0}}{\sigma L_s L_r}\right)\Delta\psi_{rq} + \left(\frac{k_{idi}}{\sigma L_s}\right)\Delta x_{sd} + \left(\frac{R_r i_{sq0}}{L_r i^*_{sd20}} - \frac{2R_r i^*_{sq10}}{L_r i^*_{sd20}} - N\omega_{m0}\right)\Delta i^*_{sq1} + \left(-\frac{R_r i_{sq0} i^*_{sq10}}{L_r {i^*_{sd20}}^2} + \frac{R_r {i^*_{sq10}}^2}{L_r {i^*_{sd20}}^2}\right)\Delta i^*_{sd2} + \left(\frac{1}{2}\frac{k_{idp}}{\sigma L^2_m}\left(\frac{2L_r(1+\sigma^2)i^*_{sq0}}{P}\right)^{-\frac{1}{2}}\right)\Delta i^*_{sq} + \left(Ni_{sq0} + \frac{NL_m\psi_{rq0}}{\sigma L_s L_r} - Ni^*_{sq10}\right)\Delta\omega_m \quad \textit{(Eq. 27)}$$

$$\frac{d}{dt}\Delta i_{sq} = \left(-N\omega_{m0} - \frac{R_r i^*_{sq10}}{L_r i^*_{sd20}}\right)\Delta i_{sd} + \left(-\frac{k_{iqp}+R_s}{\sigma L_s} - \frac{R_r(1-\sigma)}{\sigma L_r}\right)\Delta i_{sq} + \left(-\frac{NL_m\omega_{m0}}{\sigma L_s L_r}\right)\Delta\psi_{rd} + \left(\frac{L_m R_r}{\sigma L_s L_r^2}\right)\Delta\psi_{rq} + \left(\frac{k_{iqi}}{\sigma L_s}\right)\Delta x_{sq} + \left(N\omega_{m0} + \frac{R_r}{L_r}\frac{i^*_{sq10}}{i^*_{sd20}}\right)\Delta i^*_{sd1} + \left(-\frac{R_r}{L_r}\frac{i_{sd0}}{i^*_{sd20}} + \frac{(1-\sigma)R_r}{\sigma L_r} + \frac{R_r}{L_r}\frac{i^*_{sd10}}{i^*_{sd20}}\right)\Delta i^*_{sq1} + \left(\frac{R_r}{L_r}\frac{i_{sd0}i^*_{sq10}}{{i^*_{sd20}}^2} - \frac{R_r}{L_r}\frac{i^*_{sd10}i^*_{sq10}}{{i^*_{sd20}}^2} + \left(\frac{(1-\sigma)N\omega_{m0}}{\sigma}\right)\right)\Delta i^*_{sd2} + \left(\frac{k_{iqp}}{\sigma L_s}\right)\Delta i^*_{sq} + \left(-Ni_{sd0} + Ni^*_{sd0} - \frac{NL_m\psi_{rd0}}{\sigma L_s L_r} + \frac{(1-\sigma)Ni^*_{sd20}}{\sigma}\right)\Delta\omega_m \quad \textit{(Eq. 28)}$$

$$\frac{d}{dt}\Delta\psi_{rd} = \left(\frac{L_m R_r}{L_r}\right)\Delta i_{sd} + \left(-\frac{R_r}{L_r}\right)\Delta\psi_{rd} + \left(\frac{R_r}{L_r}\frac{i^*_{sq10}}{i^*_{sd20}}\right)\Delta\psi_{rq} + \left(\frac{R_r}{L_r}\frac{\psi_{rq0}}{i^*_{sd20}}\right)\Delta i_{sq1} + \left(-\frac{R_r}{L_r}\frac{i^*_{sq10}\psi_{rq0}}{{i^*_{sd20}}^2}\right)\Delta i^*_{sd2} \quad \textit{(Eq. 29)}$$

$$\frac{d}{dt}\Delta\psi_{rq} = \left(\frac{L_m R_r}{L_r}\right)\Delta i_{sq} + \left(\frac{R_r}{L_r}\frac{i^*_{sq10}}{i^*_{sd20}}\right)\Delta\psi_{rd} + \left(-\frac{R_r}{L_r}\right)\Delta\psi_{rq} + \left(-\frac{R_r}{L_r}\frac{\psi_{rq0}}{i^*_{sd20}}\right)\Delta i_{sq1} + \left(\frac{R_r}{L_r}\frac{i^*_{sq10}\psi_{rd0}}{{i^*_{sd20}}^2}\right)\Delta i^*_{sd2} \quad \textit{(Eq. 30)}$$

$$\frac{d}{dt}\Delta\omega_m = \left(-\frac{NL_m\psi_{rq0}}{JL_r}\right)\Delta i_{sd} + \left(\frac{NL_m\psi_{rd0}}{JL_r}\right)\Delta i_{sq} + \left(\frac{NL_m i_{sq0}}{JL_r}\right)\Delta\psi_{rd} + \left(-\frac{NL_m i_{sd0}}{JL_r}\right)\Delta\psi_{rq} + \left(-\frac{1}{J}\right)\Delta T_L \quad \textit{(Eq. 31)}$$

$$\frac{d}{dt}\Delta x_{sd} = [-1]\Delta i_{sd} + \left(\frac{1}{2}\frac{L_s}{L^2_m}\left(\frac{2L_r(1+\sigma^2)i^*_{sq0}}{P}\right)^{-\frac{1}{2}}\right)\Delta i^*_{sq} \quad \textit{(Eq. 32)}$$

$$\frac{d}{dt}\Delta x_{sq} = [-1]\Delta i_{sq} + [1]\Delta i^*_{sq} \quad \textit{(Eq. 33)}$$

$$\frac{d}{dt}\Delta i^*_{sd1} = \left[-\frac{1}{T_d}\right]\Delta i^*_{sd1} + \left[\frac{1}{T_d}\right]\left(\frac{1}{2}\frac{L_s}{L^2_m}\left(\frac{2L_r(1+\sigma^2)i^*_{sq0}}{P}\right)^{-\frac{1}{2}}\right)\Delta i^*_{sq} \quad \textit{(Eq. 34)}$$

$$\frac{d}{dt}\Delta i^*_{sq1} = \left[-\frac{1}{T_d}\right]\Delta i^*_{sq1} + \left[\frac{1}{T_d}\right]\Delta i^*_{sq} \quad \textit{(Eq. 35)}$$

$$\frac{d}{dt}\Delta i^*_{sd2} = \left[-\frac{1}{T_2}\right]\Delta i^*_{sd2} + \left[\frac{1}{T_2}\right]\left(\frac{1}{2}\frac{L_s}{L^2_m}\left(\frac{2L_r(1+\sigma^2)i^*_{sq0}}{P}\right)^{-\frac{1}{2}}\right)\Delta i^*_{sq} \quad \textit{(Eq. 36)}$$

With the equilibrium point as shown by $\omega_{m0} = 209.4254, i^*_{sd0} = 1,\ i^*_{sq0} = 0.23914$

3 Results and Discussions

The induction motor used in this modeling uses an induction motor with specifications, namely a three-phase induction motor, 750 W, 1410 rpm, and 4 poles. The controller parameters used in the simulation process of each method are shown in Table 1-2. [15]

Table 1. Parameters of Induction Motor

Parameter	Symbol	Value
Pole pairs	P	2
Stator Resistance	R_s	2.76 Ω
Rotor Resistance	R_r	2.9 Ω
Stator Inductance	L_s	0.2349 H
Rotor Inductance	L_r	0.2349 H
Mutual Inductance	L_m	0.2279 H

Table 2. Controller Parameters

Parameter	Symbol	Value
Kp Speed Controler	Kp	0.9
Ki Speed Controler	Ki	0.2

Modeling test by providing several reference speed inputs at 2000 rpm, 2600 rpm, and 3000 rpm.

a. Testing with 2000 rpm speed reference

The induction motor with the type used with the maximum rate of 1410 rpm experiments increasing the speed by 2000 rpm. The response of the system is shown in Fig. 2. The rise time on system response is 390.146 ms. Overshoot of the response is 0.505%. In simulations the response of the system can follow its reference speed, there are overshoots and the time required to reach a steady state.

The output current for the flux controller current i_{sd} lagging slightly behind the reference current (i_{sd}^*). Output of the system there is an immediate decrease towards the minimum current value. The response of i_{sd} current can follow its reference current (i_{sd}^*) and i_{sq} decrease after the system reaches the reference current speed from the speed

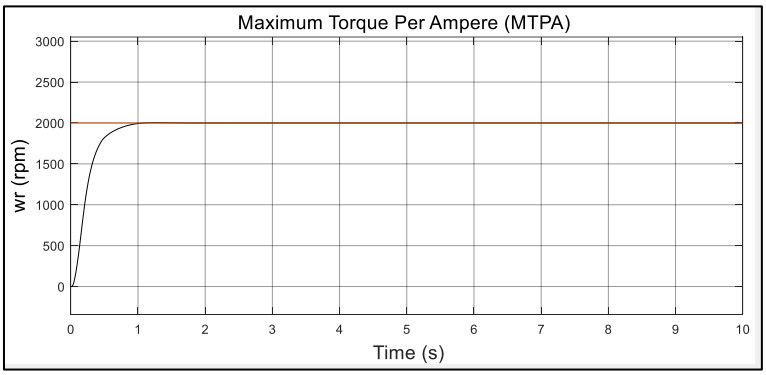


Figure 2. MTPA at 2000 rpm

controller (i_{sq}^{*}). The system is a close loop system by getting error values as input for previous improvements. The response of the system is shown in Fig 3.

b. Testing with 2600 rpm speed reference

The test was carried out by providing a reference of 2600 rpm. The response of the system is shown in Fig 4. The rise time on system response is 442,739 ms. Overshoot of the response is 4.737%. From the overshoot value, the system is safe because the overshoot is still within the tolerance limit of 0 to 10%. The response of the system can follow its reference speed, in simulations, there are overshoots and several oscillations, and the time required to reach a steady state. However, the system can reach a steady-state state.

The current i_{sd} lags behind that of i_{sd}^{*}, and oscillations occur. The response from the i_{sd} follow the reference current (i_{sd}^{*}) and can reach its steady state as shown in Fig. 5. The i_{sd} the current controller maintains with maximum current at 3A until the system reaches a speed of 2600 rpm. As for i_{sq} lagging compared to i_{sq}^{*} . The system follows the

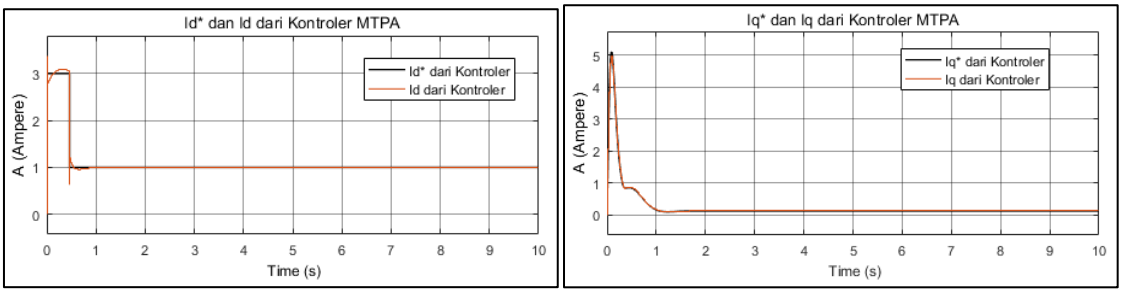


Figure 3. Comparison i_{sq}^{*} with i_{sq} and i_{sd}^{*} with i_{sd} MTPA at 2000 rpm

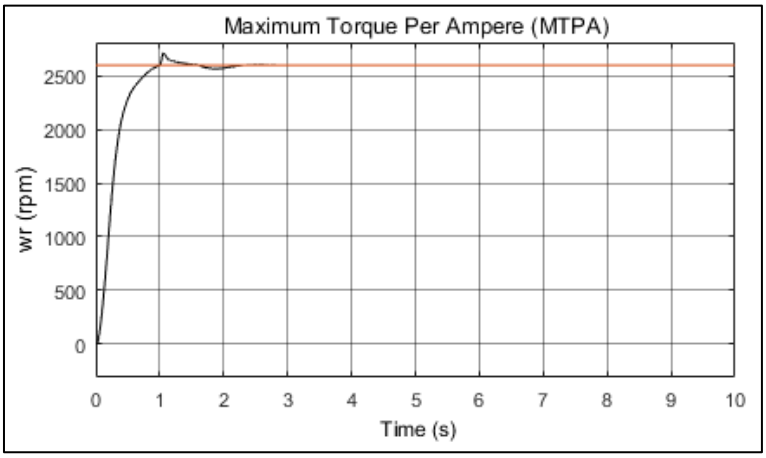


Figure 4. MTPA at 2600 rpm

references and reaches a steady-state state. The reference current undergoes oscillation and then reaches a steady-state state. The output value i_{sq} higher than the current in the previous condition. At a speed of 2600 rpm, the current controller is already at the limit of system saturation.

c. Testing with reference speed 3000 rpm.

The test was carried out by providing a reference of 3000 rpm. The response of the system cannot follow the reference speed, because the desired speed has exceeded the speed limit of the system. The system will only stay in the steady-state position even if it not reach its target speed. The response of the system is shown in Fig 6.

The current controller cannot maintain its current limit so the system failed to reach a steady-state state as shown in Fig. 7. The system continues to oscillate continuously because the system failed to reach the speed target. The desired speed exceeds the capabilities of the system so that the current from the i_{sd} still try to maintain the maximum current to reach its target speed. The condition of i_{sq} is also slightly behind

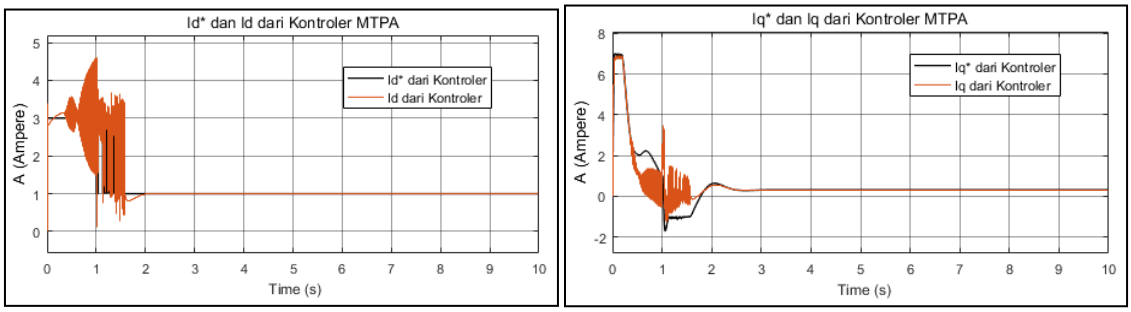


Figure 5. Comparison of i_{sq}^{*} with i_{sq} and i_{sd}^{*} with i_{sd} to MTPA i_{sd} at 2600rpm

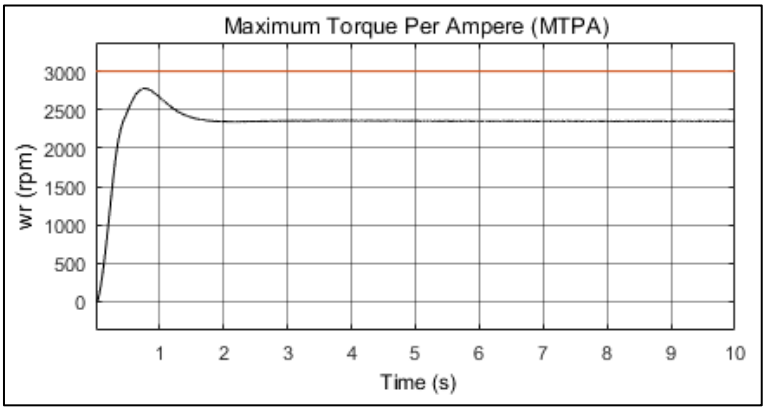


Figure 6. MTPA at 3000 rpm

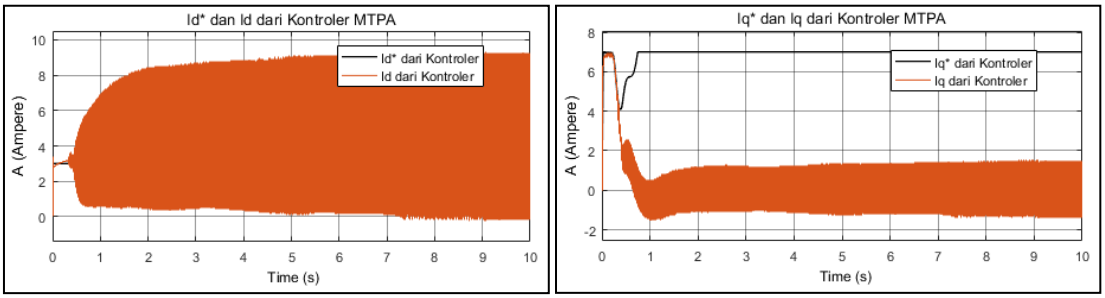


Figure 7. Comparison of i_{sd}^{*} to MTPA i_{sd} at 3000rpm

compared to i_{sq}^{*}. At first, the system followed the references, but the system failed to reach a steady-state state. The system failed to reach speed target and exceeded the system's capabilities so that the current from the i_{sq} will stop maintaining its maximum condition. The rate of the induction motor in this model is 1410 rpm. MTPA modeling can increase performance up to 2600 rpm. The modeling method with MTPA can increase performance by 84.4%

4 Conclusions

Studies on modeling with the Maximum Torque Per Ampere (MTPA) Method have been presented. The result of the modeling is that increasing the speed of each different reference input will affect settling time. The higher the speed, the longer it takes for the system to reach a steady-state state. The maximum speed that can be achieved is at a speed of 2600 rpm, so the MTPA method can increase the performance of three-phase induction motors by 84.4%. The above research is limited to the induction motor used is a squirrel cage type three-phase induction motor, and the system uses a speed sensor. The next research direction is to prove the stability of the system by analyzing pole position and movement with variations of Kp, Ki, and Kd and combining the MTPA method with other methods to improve the performance of the induction motor.

Acknowledgments

The writer expresses her thanks to God who always blessed her and to the author's family for every support that writers get. Thank you also to the thesis supervisor who has guided and supported the writer in the process of writing this journal.

References

[1]. A. Budiarto and O. Judianto, "Design of Eco-Friendly Electric Cars Based on City Car", *Jurnal Inosains Vol. 14 No. 2,*2009, pp 38-43.

[2]. M. Popescu, N. Riviere, G. Volpe, M. Villani, G. Fabri, and L. di Leonardo, "A copper rotor induction motor solution for electrical vehicles traction system," in *Proc. IEEE Energy Convers. Congr. Expo,* 2019, pp. 3924–3930.

[3]. Fauzi R and Khair J. " Direct Quadrate (DQ) Modeling on Three-Phase Induction Motor Speed Control with PI Control-Based Field Oriented Control (FOC)". *ScientiCO: Computer Science and Informatics Journal*,2018, pp. 25-35

[4]. H. Setiana, F. Husnayain and F. Yusivar, "Speed Sensorless Control of Dual Induction Motor using Direct Torque Control - Space Vector Modulation," *2019 IEEE 2nd International Conference on Power and Energy Applications (ICPEA)*, Singapore, 2019, pp. 110-114, doi: 10.1109/ICPEA.2019.8818504.

[5]. Putri. RCE and Feri Yusivar.2021. "Comparative Performance of Induction Motor Speed Controller System with Flux Weakening Control". *INCITEST 2021 "IOP Conf. Series: Materials Science and Engineering"* Vol. 1158, Iss. 1, (Jun 2021). DOI:10.1088/1757-899X/1158/1/012003

[6]. O. Wasynczuk, et. al, "A Maximum Torque per Ampere Control Strategy for Induction Motor Drives," *IEEE Transactions on Energy Conversion, Vol. 13, No. 2*, June 1998, pp. 163-169

[7]. Troy A. Nergaard, Heath E. Kouns, Jih-Sheng Lai, Charles E. Konrad, "Optimal System Efficiency Operation of an Induction Motor Drive," *in Conf. Rec. of IEEE IAS Annual Conference*, Pittsburgh, PA, Oct. 2002, pp. 826 – 831.

[8]. Harini, Bernadeta Wuri. "The Effect of Motor Parameters on the Induction Motor Speed Sensorless Control System using Luenberger Observer". 2022. *International Journal of Applied Sciences and Smart Technologies*. Volume 4, Issue 1, pages 59-74

[9]. F. Hamada, F. Husnayain and F. Yusivar, "Speed Sensorless Vector Control of Parallel Connected Induction Motor with Anti-windup Integral-Proportional Speed

Controller," *2019 IEEE 2nd International Conference on Power and Energy Applications (ICPEA)*, Singapore, pp. 89-93, doi: 10.1109/ICPEA.2019.8818527.

[10]. F. Yusivar and S. Wakao. ”Minimum requirements of motor vector control modeling and simulation utilizing CMEX S-function in MATLAB/SIMULINK”. in *4th IEEE International Conference on Power Electronics and Drive Systems.* IEEE PEDS 2001-Indonesia. (2001). *Proceedings (Cat. No.01TH8594).* pp. 315-321. doi:10.1109/PEDS.2001.975333

[11]. H. Kouns, J. -S. Lai and C. E. Konrad. ” Analysis of a traction induction motor drive operating under maximum efficiency and maximum torque per ampere conditions”. *Nineteenth Annual IEEE Applied Power Electronics Conference and Exposition APEC '04,* Anaheim, CA, USA. (2004). pp. 545-551 Vol.1, doi:10.1109/APEC.2004.1295860.

[12]. P. Naganathan and S. Srinivas, ”Maximum Torque Per Ampere Based Direct Torque Control Scheme of IM Drive for Electrical Vehicle Applications”, *IEEE 18th International Power Electronics and Motion Control Conference* (PEMC), Budapest, Hungary, 2018, pp. 256-261, doi: 10.1109/EPEPEMC.2018.8521987.

[13]. S. Peresada, S. Kovbasa, S. Dymko, and S. Bozhko, "Maximum torque-per-amp tracking control of saturated induction motors," *International Conference on Modern Electrical and Energy Systems (MEES),* Kremenchuk, Ukraine. (2017). pp. 72-75, doi: 10.1109/MEES.2017.8248955 doi:10.1109/EPEPEMC.2018.8521987

[14]. Case. M.J, “Induction Motor Reactive Power as a Means of Flux Control”, *The Transactions of The SA Institute of Electrical Engineers*.Volume: 84, Issue: 1

[15]. R. Ridwan, E. Purwanto, H. Oktavianto, M. R. Rusli, and H. Toar, “Three Phase Induction Motor Speed Control Design Using Fuzzy PID Based Indirect Field Oriented Control”, J. Integr., 11(2), 146–155, 2019.

This page intentionally left blank